

DEVELOPMENT OF A METHOD FOR  
OPTIMAL MANEUVER ANALYSIS OF COMPLEX SPACE MISSIONS

A Thesis

Presented to

the Faculty of the Department of Electrical Systems Engineering  
University of Houston

In Partial Fulfillment

of the Requirements for the Degree

Master of Science

by

Stewart F. McAdoo, Jr.

December 1973

#### ACKNOWLEDGEMENTS

I wish to recognize several persons who have contributed to the completion of this thesis. First, I am indebted to my advisor, Dr. George S. Dawkins, for his direction in the preparation of this report. Next, thanks are given to my supervisor, Jack Funk of the Mission Planning and Analysis Division (MPAD), Johnson Space Center, for his patience with my academic endeavors. A special thanks to my associate Don Jezewski, also of MPAD, for his guidance and discussions which provided much insight into the problem considered in this thesis. Last, thanks go to my wife Gayle-Ann for seeing me through this seemingly endless endeavor.

Stewart F. McAdoo, Jr.

DEVELOPMENT OF A METHOD FOR  
OPTIMAL MANEUVER ANALYSIS OF COMPLEX SPACE MISSIONS

An Abstract of a Thesis

Presented to

the Faculty of the Department of Electrical:Systems Engineering  
University of Houston

In Partial Fulfillment

of the Requirements for the Degree

Master of Science

by

Stewart F. McAdoo, Jr.

December 1973

## ABSTRACT

A system has been designed which allows mission planners to easily find optimal multiple burn space trajectories. Two previously developed methods with different gravity assumptions perform the optimization function. The power of these programs is extended by a method of costate estimation. A penalty function method of constraining coast arc times to be positive is included. The capability of the method is demonstrated by finding the optimal control for three different space missions. These include a Shuttle abort-once-around mission and two-, and three-burn geosynchronous satellite placement missions.

## TABLE OF CONTENTS

CHAPTER	PAGE
I. INTRODUCTION .....	1
II. FORMULATION OF THE MULTIBURN OPTIMIZATION PROBLEM .....	5
Differential Equation Solution .....	8
Boundary Conditions .....	9
III. CONVERGENCE TO BOUNDARY CONDITIONS .....	14
IV. STARTING ITERATES .....	16
V. EXAMPLE APPLICATIONS .....	22
Shuttle Abort-Once-Around (AOA) Mission .....	22
Synchronous Orbit Missions .....	30
VI. CONCLUSIONS AND RECOMMENDATIONS .....	45
APPENDIX - PARAMETER INEQUALITY CONSTRAINTS .....	47
REFERENCES .....	51

## LIST OF TABLES

TABLE	PAGE
I. EXAMPLE SHUTTLE AOA MISSION DATA .....	24
II. SHUTTLE AOA SOLUTION SUMMARY .....	26
III. INEQUALITY CONSTRAINT EXAMPLE .....	29
IV. EXAMPLE GEOSYNCHRONOUS ORBIT MISSION DATA .....	32
V. GEOSYNCHRONOUS MISSION SOLUTION PARAMETERS ( $T/w_I = 0.3$ ) .....	38
VI. GEOSYNCHRONOUS MISSION SOLUTION PARAMETERS ( $T/w_I = 0.2$ ) .....	40
VII. GEOSYNCHRONOUS MISSION SOLUTION PARAMETERS ( $T/w_I = 0.1$ ) .....	42

LIST OF FIGURES

FIGURE		PAGE
1.	Costate Estimation Flow Chart .....	21 .
2.	Shuttle AOA Mission Profiles	
	(a) Example 1 .....	27
	(b) Example 2, No constraint on initial coast .....	27 .
	(c) Example 2, Constrained initial coast .....	27
3.	Illustration of Geosynchronous Orbit Mission Initial and Final Orbit Geometry .....	33
4.	Illustration of Geosynchronous Orbit Mission Profiles	
	(a) 2-burn arc .....	34
	(b) 3-burn arc .....	34
5.	Performance Comparison for Various Geosynchronous Orbit Transfers .....	44

## LIST OF SYMBOLS

A	propagation matrix across burn-coast arc
c	effective exhaust velocity
d	penalty magnitude
f	function
G	gravity vector
H	Hamiltonian
h	transversality condition
I	identity matrix
J	cost function
L	thrust vector direction
M	functional relationship for initial state vector
m	mass
N	functional relationship for final state vector
n	number of thrust arcs
P	primer vector, Lagrange multiplier for acceleration constraint
p	magnitude of primer vector
Q	negative of primer vector derivative, Lagrange multiplier for velocity constraint
R	position vector
S	switch function
T	thrust magnitude
t	time
V	velocity vector

W	vector of thrust arc integrals; weighting matrix
w	weight
X	state vector, $X^T = (R^T:V^T)$
$\alpha$	control variable for thrust magnitude; vector of control variable, $\alpha^T = (P^T, -Q^T, t_1, \dots, t_{2n+1})$
$\epsilon$	Lagrange multiplier for mass
$\Delta$	incremental
$\delta$	variation
$\eta$	Lagrange multiplier for thrust magnitude constraint
$\lambda$	costate vector, $\lambda^T = (P^T:-Q^T)$
$\mu$	gravitational constant
$\nu$	Lagrange multiplier for thrust direction constraint
$\tau$	time interval
$\sum$	sum
T	coast arc state transition matrix
$\Phi$	coast arc costate transition matrix
$\Psi$	thrust arc transition matrix
$\Omega$	thrust arc transition matrix for thrust integrals
$\omega$	Schuler frequency, the constant in gravity approximation
$\nabla$	gradient operator

### Subscripts

b	burn
c	coast
F	final
I	initial
i	arc index
p	penalty

max        maximum  
x        independent variables  
y        dependent variables

Superscripts

.        time derivative  
'        used to distinguish between cost functions  
\*        optimum  
[i]      arc index for matrices  
-1       inverse  
T        transpose

## Chapter I

### INTRODUCTION

In order to reduce the high cost of space flight, thrusting maneuvers and orbit parameters must be planned so that missions are performed in an efficient manner. As missions become more complex and require more maneuvers to accomplish the mission goals, and as spacecraft thrust levels are reduced to lower vehicle cost, it becomes increasingly difficult for mission planners to determine an efficient mission plan.

Numerous computer programs have been developed which, under various assumptions and restrictions, are intended to aid the mission planner. A large number of these programs make the assumption that maneuvers to change the shape and size of the spacecraft's orbit are made impulsively (i.e., the maneuver is assumed to be an instantaneous change in velocity). The assumption of an impulsive maneuver is valid when the spacecraft thrust level is high enough that the actual time required to make the maneuver is small with respect to the total mission time. Perhaps the most general of these programs is the one described by Jezewski and Rozendaal (ref. 1). This program requires only initial and final conditions and will produce a mission profile which gives the optimum number, placements, directions, and sizes of the impulsive maneuvers.

Various approaches have been applied to the problem of analyzing missions for spacecraft which have thrust levels low enough that the impulsive thrusting approximation is not valid. One approach is to assume a near optimum guidance algorithm and numerically integrate the equations of

2

motion through thrusting maneuvers (e.g., ref. 2). Another approach is to assume a behavior for the vehicle controls and directly optimize the parameters which describe that behavior (e.g., ref. 3).

Brown, Harrold, and Johnson (ref. 4) applied the principles of optimal control to the problem of multiple burn spacecraft trajectories. The result was a method by which optimum multiple burn trajectories could be found by determining the times at which the rocket engine should be switched on and off and by determining initial values for the differential equations describing the behavior of the costate vector. The costate vector is the vector of Lagrange multipliers which adjoins the equations of motion of the state vector to the performance functional and which describes the optimal thrust vector control through each maneuver. Tarbet (ref. 5) extended the versatility of the Brown, Harrold, and Johnson program by applying a conjugate gradient algorithm as the iteration scheme for determining the optimal control. The control consists of an initial costate vector and an engine switch time array. To assist mission planners in determining starting values for the costate and switch times for the iteration process, Tarbet first computed an optimum impulsive solution to the problem by the method described in reference 1 and formed thrust arcs around the impulses according to the technique described in reference 6. Although Tarbet's program successfully found solutions to problems, it was of limited usefulness because numerical integration of state, costate, and perturbation differential equations across thrust arcs required a significant amount of computer time for many problems and because the scheme for determining starting iterates was not suitable for problems in which the spacecraft thrust level was low.

Recently, Jezewski (ref. 7), in an effort to reduce the time required for computing multiburn trajectories, produced a program based on the principles of optimal control similar to the Brown, Harrold, and Johnson program except that he made the assumption that the gravitational acceleration vector varies linearly with the radius vector. This assumption resulted in a closed form solution to the state and costate differential equations across the thrust arcs which greatly reduced the trajectory computation time.

Tarbet's version of the Brown, Harrold, and Johnson program and Jezewski's program would complement each other if combined. Jezewski's program can be used to provide a starting iterate for Tarbet's program since the two programs are similarly structured. A starting iterate obtained from Jezewski's program would not have limitations imposed by the thrust level; and because it is obtained from a finite thrust program, it would be more accurate than the method of forming thrust arcs around impulses. The most obvious result of the increased accuracy would be the reduction in computer time required. Another advantage would be the ability of the combined programs to find solutions to missions performed by spacecraft having low thrust levels, for which solutions were previously not possible. On the other hand Jezewski's program is in itself sufficiently accurate for a large number of applications, and Tarbet's program could be used to verify that accuracy when necessary. Thus, the use of Jezewski's program followed by verification of certain important solutions with Tarbet's program would allow parametric studies related to mission planning without entailing a large amount of computer time. Described herein is the development of such a combination.

Because there is still a requirement to estimate the initial costate vector and the engine switch times, mission planners may have difficulty applying the program successfully. It is expected that the mission planner can estimate with reasonable accuracy the array of engine switch times. The theory applied in references 5 and 7 proves that on an optimal trajectory the spacecraft thrust vector is aligned with the first three components of the costate vector (called the primer vector). With this in mind, the engineer can make some estimate of the direction of the primer vector. The last three components of the costate vector, which are called the primer vector derivative, cannot be estimated by association with physical properties of the mission under consideration. In this study, a scheme will be presented which is derived from Jezewski's work for estimating the primer vector derivative. This scheme will require the planner to make some estimate of engine switch times and estimate roughly the direction the thrust vector should be oriented at the start of each thrust arc (e.g., along the velocity vector, normal to the orbit plane, etc.). An initial costate vector based on these estimates will be generated and will be passed on to the optimization program, which is composed of Jezewski's and Tarbet's program. To demonstrate the versatility of the program, several examples of solutions to missions of interest will be presented. The optimal control for three different space missions will be given. These include a Shuttle abort-once-around mission and two- and three-burn geosynchronous satellite placement missions.

## Chapter II

## FORMULATION OF THE MULTIBURN OPTIMIZATION PROBLEM

The multiburn space trajectory optimization problem is to find a set of thrusting and coasting arcs which minimizes some performance functional while transferring between two physical boundary conditions,

$$M(R_I, V_I, t_I) = 0 \quad (1)$$

and

$$N(R_F, V_F, t_F) = 0 \quad (2)$$

subject to the differential constraints

$$\dot{R} = V \quad (3)$$

$$\dot{V} = G + \frac{T}{m} L \quad (4)$$

$$\dot{m} = - \frac{T}{c} \quad (5)$$

where  $R$ ,  $V$ , and  $m$  are the state variables and  $T$  and  $L$  are the control variables.  $R$  and  $V$  are, respectively, radius and velocity vectors in Cartesian coordinates. The constraint on thrust magnitude

$$0 \leq T \leq T_{\max} \quad (6)$$

is required as is the constraint on the thrust direction vector,  $L$ , that

$$L^T L = 1 \quad (7)$$

References 4 and 7 base their solution to the  $n$ -burn optimization problem on the functional

$$J = \int_{t_I}^{t_F} - \dot{m} dt \quad (8)$$

which is to be minimized. Notice that minimizing this functional is equivalent to minimizing mass loss or, alternatively, maximizing final mass. The conditions needed for optimal control of a multiburn trajectory are developed in the literature (refs. 4, 5, 7) and the development is presented herein for the convenience of the reader.

The inequality constraint (6) is first rewritten

$$T(T_{\max} - T) - \alpha^2 = 0 \quad (9)$$

The constraints (3), (4), (5), (7), and (9) are adjoined to (8) to form the variational Hamiltonian

$$H = -\dot{m} + Q^T V + P^T \left( G + \frac{T}{m} L \right) + \epsilon \dot{m} + \nu (1 - L^T L) + \eta [T(T_{\max} - T) - \alpha^2] \quad (10)$$

where  $Q$ ,  $P$ ,  $\epsilon$ ,  $\nu$ , and  $\eta$  are Lagrange multipliers adjoining the constraints to the functional. The necessary conditions for optimality with respect to the control  $L$  are given by

$$\frac{\partial H}{\partial L} = 0 = P^T \frac{T}{m} - 2\nu L \quad (11)$$

By solving the set of linear equations (11) the necessary conditions are satisfied if

$$L = \pm \frac{P}{p} \quad (12)$$

The choice of which sign to use in equation (12) is determined by applying the Weierstrass E- condition, which requires that the Hamiltonian on the extremal curve be greater than the Hamiltonian on any nearby admissible curve for an extremum to occur. This implies that

$$\frac{\partial^2 H}{\partial L^2} \leq 0 \quad (13)$$

By application of (13), it follows that

$$L = + \frac{P}{p} \quad (14)$$

Substituting (14) into (10),  $-c\dot{m}$  for  $T$ , and rearranging, the Hamiltonian becomes

$$H = -\dot{m}(1 - \epsilon + p \frac{c}{m}) + Q^T V + P^T G + \eta [T(T_{\max} - T) - \alpha^2] \quad (15)$$

The term  $\alpha$  is a control variable, so  $\frac{\partial H}{\partial \alpha} = 0$  is a necessary condition.

$$\frac{\partial H}{\partial \alpha} = -2\eta\alpha = 0 \quad (16)$$

Either  $\eta$  or  $\alpha$  must equal zero. The Lagrange multiplier  $\eta$  cannot in general be assumed to be zero. From equation (9), for  $T=0$  and  $T = T_{\max}$ ,  $\alpha$  must equal 0. By making the assumption that the thrust can only take on values of zero and  $T_{\max}$ , the quantity in brackets becomes equal to zero, and the last term of (15) then can be deleted so that the Hamiltonian becomes

$$H = -\dot{m}(1 - \epsilon + p \frac{c}{m}) + Q^T V + P^T G \quad (17)$$

The necessary conditions for optimality with respect to the multipliers  $P$ ,  $Q$ , and  $\epsilon$  are

$$\dot{P}^T = - \frac{\partial H}{\partial V} = -Q^T \quad (18)$$

$$\dot{Q}^T = - \frac{\partial H}{\partial R} = -(P^T V)G \quad (19)$$

and

$$\dot{\epsilon} = - \frac{\partial H}{\partial m} = T \frac{P}{m^2} \quad (20)$$

### Differential Equation Solution

Equations (3), (4), (5), (14), (18), (19), and (20) compose a set of differential equations which must be solved to find the optimal multiple burn trajectory.

Coast arcs.- On coasting arcs both reference 4 and 7 assume that the gravitational vector  $G$  is given by the inverse-square relation

$$G_c = - \frac{\mu R}{|R|^3} \quad (21)$$

For an inverse-square gravitational field, the solutions for the state and costate vectors are known in closed form (refs. 8 and 4) and may be expressed as

$$X(\tau) = TX(0) \quad (22)$$

$$\lambda(\tau) = \Phi\lambda(0) \quad (23)$$

where  $T$  and  $\Phi$  are known 6-by-6 matrices.

Thrust arcs.- Reference 4 assumes that the gravitational vector  $G$  is also given by equation (21). No solution for the equations of motion in closed form exists assuming this gravitational vector. The solution across thrust arcs is found by using numerical integration.

Reference 7 makes a different assumption for  $G$  on thrust arcs. To facilitate the solution of the differential equations the assumption that

$$G_b = -\omega^2 R \quad (24)$$

is made so that equations (3), (4), (18), and (19) can be solved in closed form. The term  $\omega$  in equation (24) is defined by

$$\omega = \sqrt{\frac{\mu}{|R|^3}} \quad (25)$$

where  $|R|$  is evaluated only at the start of the thrust arc. The solution for equations (3) and (4) is

$$X(\tau) = \Psi X(0) + \Omega W \quad (26)$$

and the solution for equations (18) and (19) is

$$\lambda(\tau) = \Psi \lambda(0) \quad (27)$$

where

$$\Psi = \begin{bmatrix} I \cos \omega \tau & I \frac{1}{\omega} \sin \omega \tau \\ -I \omega \sin \omega \tau & I \cos \omega \tau \end{bmatrix} \quad (28)$$

$$\Omega = \frac{T}{\omega} \begin{bmatrix} I \sin \omega \tau & -I \cos \omega \tau \\ I \omega \cos \omega \tau & I \sin \omega \tau \end{bmatrix} \quad (29)$$

where  $I$  is an identity matrix of dimension 3, and

$$W = \begin{bmatrix} \int_0^T \frac{P}{m(t)_p} \cos \omega \tau dt \\ \int_0^T \frac{P}{m(t)_p} \sin \omega \tau dt \end{bmatrix} \quad (30)$$

#### Boundary Conditions

To complete the solution to the multiburn optimization problem, a set of initial values for the state variables  $R, V, m$  and the variables  $P, Q, \epsilon$  must be obtained. In addition, another set of variables, the set of engine switch times  $t_1, \dots, t_{2n+1}$ , where  $n$  is the number of thrust arcs, must be determined. Indexing for the switch times is as follows:  $t_0$  is the time at which the vehicle is in the initial state

given by equation (1);  $t_{2i-1}$  is the time of the start of the  $i$ th thrust arc;  $t_{2i}$  is the time of the termination of the  $i$ th thrust arc; and  $t_{2n+1}$  is the time of termination of a final coast arc which is required to obtain an optimum time-open transfer.

Equation (1) gives values for the state variables  $R$  and  $V$ , and the initial value of  $m$  will be specified according to the characteristics of the vehicle performing the mission. The variables  $P, Q, \epsilon, t_1, \dots, t_{2n+1}$  ( $2n + 8$  in all) must be determined by satisfaction of boundary conditions. The following derivation of a set of boundary conditions is taken from unpublished notes by Jezewski.

Six boundary conditions are obtained from equation (2). Of the remaining  $2n+2$  conditions,  $2n+1$  are obtained from conditions of optimality that are imposed on the Hamiltonian, equation (17). The conditions of optimality on  $H$  are (1)  $H$  must be constant across the trajectory, (2)  $H$  must be maximized, and (3) for a time-open solution,

$$H_{2n+1} = 0 \quad (31)$$

Finally, the condition

$$\lambda_I^T \lambda_I = \text{constant} \neq 0 \quad (32)$$

is required because of the homogeneous property of the costate differential equations.

Equation (17) is rewritten

$$H = -\dot{m}S + h \quad (33)$$

where

$$h = P^T G + Q^T V \quad (34)$$

is called the transversality condition and

$$S = 1 - \epsilon + \frac{cP}{m} \quad (35)$$

The term  $S$  is called the switch function because the decision whether  $\dot{m} = 0$  or  $\dot{m} = \dot{m}_{\max}$  may be based on the sign of  $S$ . When  $S$  is negative, a value of  $\dot{m}$  equal to  $\dot{m}_{\max}$  would reduce the value of  $H$  (remember that  $\dot{m}_{\max}$  is a negative number) which is to be maximized. When  $S$  is negative, then  $\dot{m}$  must equal zero. It follows, then, that at each engine switch time  $S$  must equal zero. The following boundary conditions result:

$$S_i = 0 \quad i = 1, \dots, 2n \quad (36)$$

Equations (2), (31), (32), and (36) then define the required  $2n+8$  boundary conditions. Experience, however, indicates that these conditions are unsatisfactory because of the sensitivity of the switch function and because of the requirement to integrate the equation for  $\epsilon$  [eq. (20)]. Manipulation of the conditions of equation (36) along with the constancy of  $H$  will eliminate  $\epsilon$  from the solution. Elimination of  $\epsilon$  from the solution reduces the number of unknown variables to  $2n+7$  and, therefore, the number of boundary conditions required to  $2n+7$ .

Equations (5) and (20) show that, since  $T$  equals zero on coast arcs,  $m$  and  $\epsilon$  are constant on coast arcs. Solving the equation for  $S_{2i}$  for  $\epsilon$  and substituting the result into the equation for  $S_{2i+1}$  give

$$S_{2i+1} = 0 = 1 - \left(1 + \frac{cp_{2i}}{m}\right) + \frac{cp_{2i+1}}{m} \quad i = 1, \dots, n-1 \quad (37)$$

Simplification of equation (37) gives the conditions

$$p_{2i} = p_{2i+1} \quad i = 1, \dots, n-1 \quad (38)$$

which states that the magnitude of the primer vector at the end of each interior coast arc is the same as at the beginning of that coast arc.

As can be easily shown, on coast arcs  $H$  is constant; however, only on an optimum trajectory is  $H$  constant across the entire multi-burn trajectory. On an optimum trajectory, then  $H$  must have the same value at the beginning and end of each thrust arc in order to satisfy the condition that  $H$  be a constant.

$$H_{2i} - H_{2i-1} = -\dot{m}S_{2i} + h_{2i} + \dot{m}S_{2i-1} - h_{2i-1} = 0 \quad i = 1, \dots, n \quad (39)$$

At the beginning and end of each thrust arc,  $S_{2i}$  and  $S_{2i-1}$  must be equal to zero; thus, equation (39) reduces to

$$h_{2i} - h_{2i-1} = 0 \quad i = 1, \dots, n \quad (40)$$

Equation (38) satisfies the condition on the switch function given in equation (36) for  $i = 2, \dots, 2n-1$ . To verify the satisfaction of equation (36) for  $i = 1$ , equation (39) should be examined for  $i = 1$ .

$$-\dot{m}S_2 + h_2 + \dot{m}S_1 - h_1 = 0 \quad (41)$$

Since  $S_2$  is forced to be equal to zero by condition (38), equation (41) can be rewritten

$$\dot{m}S_1 + (h_2 - h_1) = 0 \quad (42)$$

According to equation (40),  $h_2 - h_1$  is equal to zero, so  $S_1$  must equal zero. Similarly, since  $S_{2n-1} = 0$  by equation (38), equation (39) can be rewritten for  $i = n$ ,

$$\dot{m}S_{2n} + (h_{2n} - h_{2n-1}) = 0 \quad (43)$$

Equation (40) requires that  $(h_{2n} - h_{2n-1}) = 0$ ; therefore,  $S_{2n}$  must also equal zero. The boundary conditions of equations (38) and (40) then satisfy the conditions stated in equation (36). Equations (2), (31), (32), (38), and (40) form a complete set of  $2n+7$  boundary conditions which may be used to determine the  $2n+7$  variables  $P, Q, t_1, \dots, t_{2n+1}$ .

When the gravity approximation [eq. (24)] is made on thrust arcs, the switch function at the end of each thrust arc must be modified to account for the discontinuity in the gravitational vector, so

$$S = 1 + \epsilon + \frac{c_p}{m} + \frac{P^T(G_b - G_c)}{\dot{m}_{\max}} \quad (44)$$

and the boundary condition (38) becomes

$$0 = p_{2i} - p_{2i+1} - \frac{m_{2i}}{c\dot{m}_{\max}} P_{2i}^T (G_b - G_c) \quad (45)$$

In summary, the multiburn trajectory optimization problem has been formulated as a boundary value problem in the  $2n+7$  unknown quantities  $P, Q, t_1, \dots, t_{2n+1}$  with the differential equations (3), (4), (5), (18), and (19) and with the  $2n+7$  boundary conditions given in equations (2), (31), (32), (38), and (40).

## Chapter III

## CONVERGENCE TO BOUNDARY CONDITIONS

After solutions to the differential equations have been obtained, what remains is a set of  $2n+7$  nonlinear equations in the  $2n+7$  unknown parameters  $P, Q, t_1, \dots, t_{2n+1}$ . Evaluating these nonlinear equations requires the computation of a trajectory for which a set of values for the unknowns is given. In general, an initial estimate for the unknowns will not yield the desired solution to the nonlinear equations. An iterative convergence process is required to obtain a set of values for the  $2n+7$  unknowns which produces the desired solution. One method of accomplishing this is to create a cost function and determine values of the parameters for which the cost function is minimized. One cost function is

$$J' = f(\alpha)^T f(\alpha) \quad (46)$$

where  $f(\alpha)$  is the vector function of the unknown parameters

$$\alpha^T = (P^T, -Q^T, t_1, \dots, t_{2n+1}) \quad (47)$$

For the solution in which the inverse-square gravity model of equation (21) is assumed on all arcs the matrix of partial derivatives,  $\frac{\partial f}{\partial \alpha}$ , is known (in the sense that differential equations for  $\delta \dot{X}$  and  $\delta \lambda$  must be numerically integrated on thrust arcs) and is described in reference 4. Reference 7 gives the matrix  $\frac{\partial f}{\partial \alpha}$  for the solution in which the gravity approximation of equation (24) is made on thrust arcs. With this information, a number of algorithms are applicable to this problem. Tarbet (ref. 5) applied a conjugate gradient algorithm to the full inverse-square problem of reference 4 with good results.

The algorithm described in reference 9 was used in the program of reference 7. (This program will be referred to as the  $\omega$  program.) That algorithm has been modified as shown in the appendix to increase the capability of the program. This enhancement was motivated in part by the requirement that the thrusting arcs and intermediate coasting arcs be non-negative, which results in a parameter inequality constraint. The constraint capability was extended to initial and final coast arcs as mission requirements dictated.

## Chapter IV

## STARTING ITERATES

In order to find a solution to the problem, an initial estimate for  $\alpha$  must be supplied. In the program described in reference 5, an impulsive solution and finite thrust arcs created about each impulse make up the starting iterate for the multiburn optimization program. Because of the inaccuracies inherent in approximating an impulse with a finite thrust arc, this method is restricted to relatively high (greater than 0.3) thrust-to-weight ratios. However, since appreciable amounts of computer time are required to find a solution, particularly for problems having long thrust arcs, an accurate estimate for  $\alpha$  must be obtained. The  $\omega$  program can be used to determine a starting value for  $\alpha$  for the full inverse-square program because its closed-form trajectory computation permits rapid convergence. When these two programs are combined so that the  $\omega$  program is first used to obtain a starting iterate for the full inverse square program, a very versatile optimal maneuver analysis program results. The  $\omega$  program can be used for preliminary mission studies and performance scans, since its rapid convergence allows such studies without excessive computer time requirements. When more accurate data or verification of data from the  $\omega$  program are required, then the inverse-square program can be used.

In order to initialize the iteration loop in the  $\omega$  program, an estimate of costate,  $\lambda$ , and the engine on and off times must be provided. It

is expected that a mission engineer, relying on past experience and a knowledge of the desired trajectory can estimate the engine on and off times. The costate is a six-dimensional vector comprised of a primer vector  $P$  and its derivative  $\dot{P}$ .

$$\lambda = \begin{pmatrix} P \\ \dot{P} \end{pmatrix} \quad (48)$$

where  $\dot{P} = -Q$ . According to (14), the thrust acceleration vector is aligned with and has the same direction as the primer vector,  $P$ . Thus, knowing what is to be accomplished in a particular maneuver, a mission engineer can estimate how the thrust vector should be directed (e.g., posigrade or retrograde) and, therefore, the direction of the primer vector,  $P$ . If some estimate for  $|P|$  at the start of each maneuver can be made, then the primer derivative,  $\dot{P}$ , is the only quantity for which an estimate is not readily obtained. Reference 10 has a scheme for the estimation of  $\dot{P}$  for two-burn maneuvers. The following is an extension of that scheme to  $n$  burns.

According to equation (27), the costate  $\lambda_2$  at time  $t_2$  at the end of a burn may be computed in terms of  $\lambda_1$  at  $t_1$  the beginning of the burn by

$$\lambda_2 = \Psi \lambda_1 \quad (49)$$

where  $\Psi$  is a matrix which is a function of time only. Similarly, across coast arcs  $\lambda_3$  can be expressed in terms of  $\lambda_2$  as

$$\lambda_3 = \Phi \lambda_2 \quad (50)$$

according to equation (23). Combining equations (49) and (50) gives

$$\lambda_3 = \Phi\Psi\lambda_1 \quad (51)$$

which is the solution for the costate at the beginning of the second burn arc of a multiburn solution, the time at which another estimate for  $P$  can be made. For conciseness, define

$$A^{[i]} = \phi^{[i]}\psi^{[i]} \quad (52)$$

on the  $i$ th burn-coast arc, and renumber  $\lambda$  so that  $\lambda_i$  is the value at the beginning of the  $i$ th burn-coast arc,

$$\lambda_{i+1} = A^{[i]}\lambda_i \quad (53)$$

and rewrite equation (53)

$$\begin{bmatrix} P_{i+1} \\ \dot{P}_{i+1} \end{bmatrix} = \begin{bmatrix} A_{11}^{[i]} & A_{12}^{[i]} \\ A_{21}^{[i]} & A_{22}^{[i]} \end{bmatrix} \begin{bmatrix} P_i \\ \dot{P}_i \end{bmatrix} \quad (54)$$

$\dot{P}_i$ , when  $i=1$  is the quantity to be estimated. Two equations involving  $\dot{P}_i$  can be written from equation (54)

$$P_{i+1} = A_{11}^{[i]}P_i + A_{12}^{[i]}\dot{P}_i \quad (55)$$

and

$$\dot{P}_{i+1} = A_{21}^{[i]}P_i + A_{22}^{[i]}\dot{P}_i \quad (56)$$

Equation (55) can be solved directly for  $\dot{P}_i$ :

$$\dot{P}_i = A_{12}^{[i]-1} \left( P_{i+1} - A_{11}^{[i]}P_i \right) \quad (57)$$

which gives an estimate for  $\dot{P}_i$ , for a two-burn problem, by setting  $i=1$ . Solving equation (56) for  $\dot{P}_i$  gives

$$\dot{P}_i = A_{22}^{[i]-1} \left( \dot{P}_{i+1} - A_{21}^{[i]} P_i \right) \quad (58)$$

With proper indexing, equation (57) is a solution for  $\dot{P}_{i+1}$ ; so substituting equation (57) into equation (58) yields

$$\dot{P}_i = A_{22}^{[i]-1} \left[ A_{12}^{[i+1]-1} \left( P_{i+2} - A_{11}^{[i+1]} P_{i+1} \right) - A_{21}^{[i]} P_i \right] \quad (59)$$

For  $i=1$ , equation (59) provides an estimate for  $\dot{P}_1$  for a three-burn solution. Proceeding similarly, an estimate for a four-burn problem can be obtained by substituting equation (59) into equation (58):

$$\dot{P}_i = A_{22}^{[i]-1} \left\{ A_{22}^{[i+1]-1} \left[ A_{12}^{[i+2]-1} \left( P_{i+3} - A_{11}^{[i+2]} P_{i+2} \right) - A_{21}^{[i+1]} P_{i+1} \right] - A_{21}^{[i]} P_i \right\} \quad (60)$$

Examination of equations (57), (59), and (60) indicates that a form exists for a  $\dot{P}_1$  estimate in terms of the estimates for the  $P$  vectors at the start of each burn-coast arc and that the equations lend themselves to a computer solution for  $\dot{P}_1$  for a trajectory with a desired number of burn arcs. To implement this procedure a trajectory must be calculated by using the time estimates and some guess made for  $P_1$  and  $\dot{P}_1$  to obtain the  $A^{[i]}$  matrices. Usually  $P_1$  is specified to be a vector of unit magnitude in the desired thrust direction and  $\dot{P}_1$  is chosen to be a unit vector in the gravity acceleration direction. Given  $P_1$  and  $\dot{P}_1$  a trajectory is propagated and the state vectors, the costate vectors, and the  $A^{[i]}$  are computed and saved. The desired  $P_i$  vectors are computed based on the just-saved state vectors and the mission engineer's estimate of the required direction for the  $P$  vectors. These desired  $P$  vectors

are then compared with those actually computed in the trajectory propagation. If any of the  $P_i$  are greater than a given tolerance in direction (about 0.6 radians), a new  $\dot{P}_1$  estimate is calculated from the equations developed previously using the  $A^{[i]}$  matrices and the desired  $P_i$  vectors. A new trajectory is then calculated by starting the iterative loop again. A functional flow chart for the estimation scheme is given in figure 1.

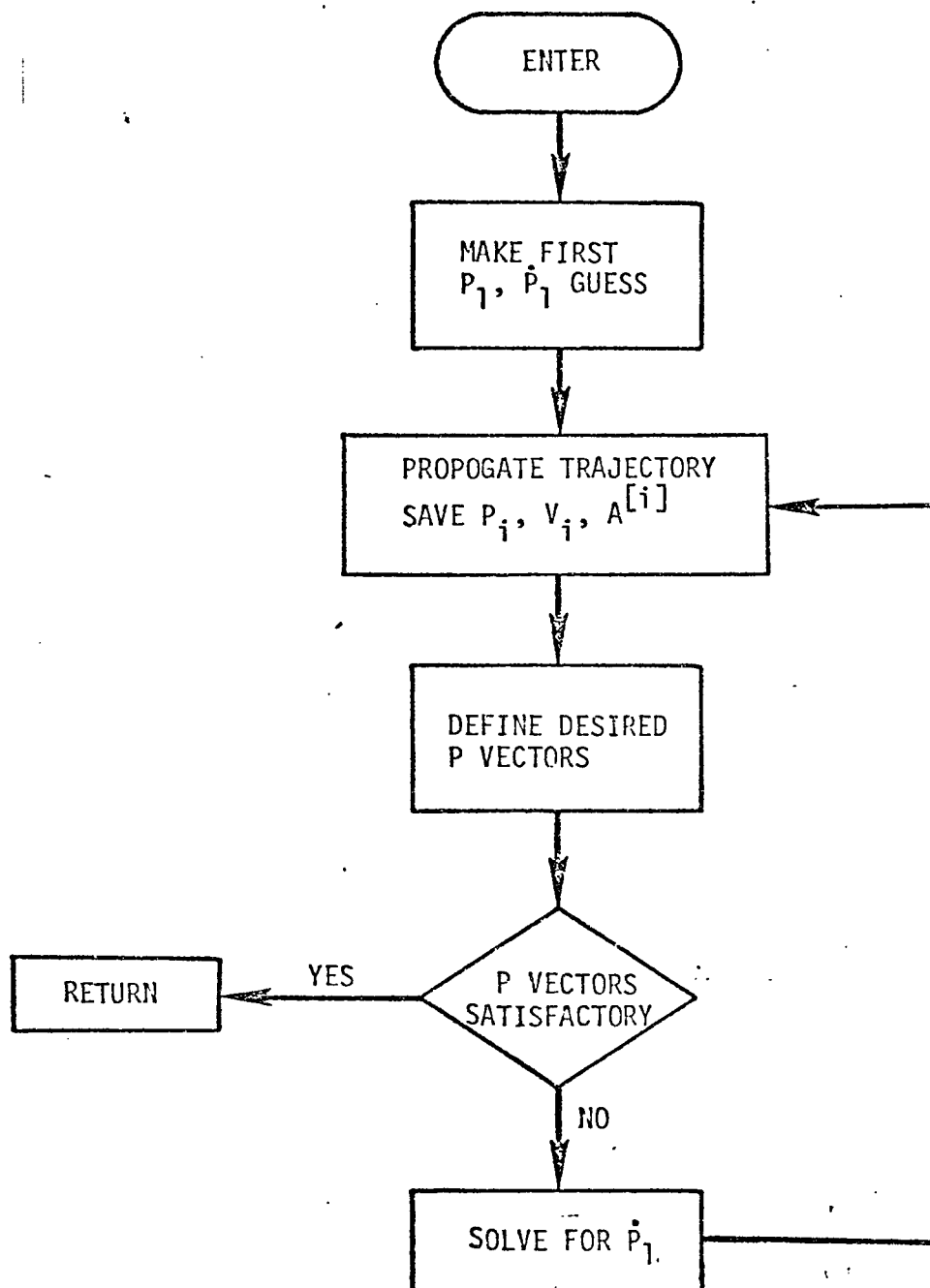


Figure 1.- Costate estimation flow chart.

## Chapter V

### EXAMPLE APPLICATIONS

The program (called OPBURN) described in the foregoing sections is very versatile. It allows mission planners to determine optimal multiple burn trajectories for a large class of orbital transfer problems. They need to provide the program only with data describing the initial and final conditions, the vehicle characteristics, and a rough idea of some of the physical characteristics of the solution. To demonstrate the program capability, solutions to two types of example problems will be presented. The first type of problem is a Shuttle abort-once-around (AOA) trajectory from the suborbital tank staging point to the entry interface conditions. The second type of problem for which solutions will be presented is a geosynchronous satellite placement mission which is initiated from a low-altitude circular orbit.

#### Shuttle Abort-Once-Around (AOA) Mission

Current plans for the launch of the Space Shuttle are to shut down the main engines before a safe orbit has been attained, separate the external tank from the orbiter so that it will return to earth without needing a retrorocket, and then continue the injection of the orbiter with the orbit maneuvering system (OMS) engines. Should an abort become necessary at the tank separation point, the current plan is to make a circumnavigation of the earth by using OMS maneuvers to ensure that the proper entry interface for a safe landing is achieved. For certain

missions this will be the nominal profile. One of the design missions for the Shuttle is a single orbit mission in which the Shuttle is launched and transfers to a suitable low-altitude orbit (e.g., approximately 100 n. mi. altitude circular orbit), dispenses a payload, deorbits, re-enters, and lands at its departure point all in one orbit. This mission is to be flown from the Western Test Range and the orbit will have an inclination of  $104^\circ$ .

The OPBURN program was used to analyze the OMS propulsion requirements for this mission when the suborbital tank staging launch scheme was employed. The state vectors (R and V) were specified at the main engine cutoff and at the reentry interface, the vehicle characteristics were defined, and the program OPBURN was used to determine a sequence of two burns to achieve a transfer between the two states. The state vectors and the vehicle characteristics for the example are given in table I. Note that two final state vectors are given. The solution to the AOA mission having the first given final state vector will include the full inverse square solution from the final phase of the program. To demonstrate the inequality constraint capability of OPBURN, solutions to the AOA mission having the second given final state vector will be presented with and without imposition of an inequality constraint on the initial coast arc. While the mission has a  $104^\circ$  inclination, it is completely coplanar, so for simplicity, the problem was formulated for OPBURN in the equatorial plane. Note that the vehicle thrust-to-weight ratio is very small (0.049). In addition to the data in table I, the thrust direction at the start of the first burn arc was specified to be posigrade, while the thrust direction at the start of the second burn arc was retrograde. An estimate of engine on and off times was provided.

TABLE I  
EXAMPLE SHUTTLE AOA MISSION DATA

	<u>State Vectors</u>		
	<u>Initial</u>	<u>Final</u>	
		<u>Example 1</u>	<u>Example 2</u>
Radius, ft	21 229 538.0	21 295 738.0	21 295 738.0
Right Ascension, deg	13.2	258.5	261.5
Declination, deg	0	0	0
Velocity, fps	25 700.0	25 650.0	25 700.0
Flight-path angle, deg	0.2	-0.715	-0.815
Azimuth, deg	90.0	90.0	90.0

Vehicle characteristics

Initial weight, lb	243 031.0
Thrust, lb	12 000.0
Specific impulse, sec	313.2

Table II gives data describing the solution to the first AOA problem. The times shown in column 1 are those provided the program as input data. The costate vector in column 1 is produced by the costate estimation routine, and the orbital parameters which follow it describe the orbits and thrust arcs which result from state propagation using that costate estimate. Using the solution described in column 1 as the starting iterate, the  $\omega$  program converged in 13 iterations. Parameters describing that solution are given in column 2 of table II. Note that the initial coast length was increased by approximately 87 seconds. The first thrust arc was increased by 15 seconds, and the second thrust arc was delayed for approximately 300 seconds and increased 13 seconds in duration. The costate vector, however, was changed only slightly in obtaining the converged solution. When the converged solution from the  $\omega$  program was used as a starting point, the inverse-square program converged in 11 iterations. Parameters describing that solution are also listed in table II. The similarity of the  $\omega$  and inverse-square solutions indicates that at least for this class of problem the  $\omega$  program has sufficient accuracy to preclude the need of the inverse-square program for every desired solution. An altitude profile of this mission is shown in figure 2(a).

TABLE II  
SHUTTLE AOA SOLUTION SUMMARY

		<u>Initial estimate</u>	<u><math>\hat{\omega}</math> approximation</u>	<u>Inverse-square solution</u>
Engine switch time array, sec	$t_0$	0	0	0
	$t_1$	1	87.7	87.8
	$t_2$	95	166.8	166.9
	$t_3$	2413	2711.6	2711.6
	$t_4$	2460	2771.7	2771.8
Costate		-.226	-.271	-.271
		.974	.854	.854
		0	0	0
		-.385	-.443	-.443
		-.127	-.033	-.033
		0	0	0
Intermediate orbit				
Perigee altitude, n. mi.		48.2	49.3	49.3
Apogee altitude, n. mi.		106.8	92.4	92.5
$\Delta V_1$ , fps		150.4	126.5	126.4
$\Delta V_2$ , fps		76.1	97.2	97.4
$\sum \Delta V$ , fps		226.5	223.7	223.8

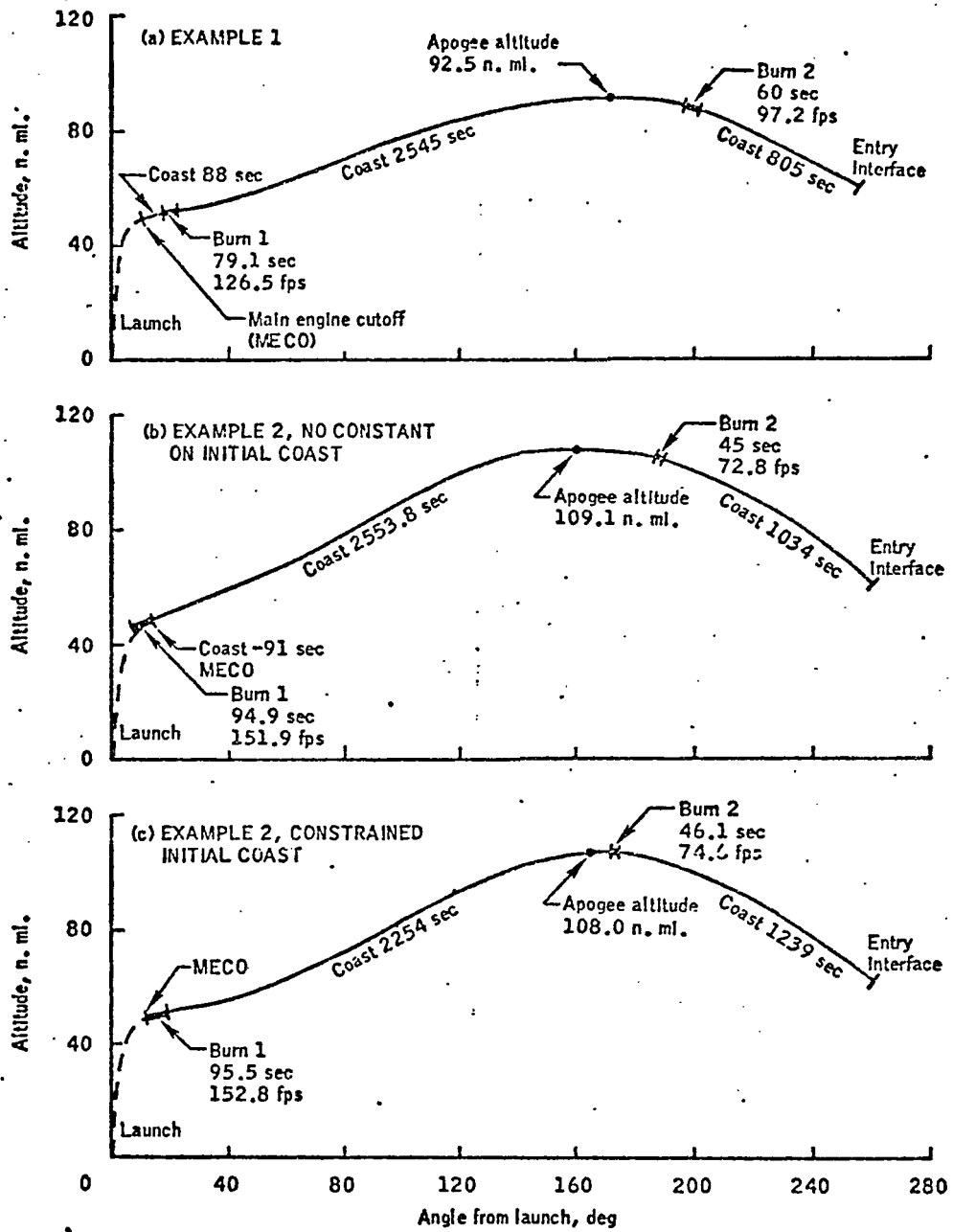


Figure 2.- Shuttle AOA mission profiles.

The  $\omega$  program is formulated to determine the optimum transfer between the two orbits specified by the input initial and final state vectors. By determining the length of the coast arcs before the first burn and after the last burn while allowing their length to be either positive or negative, departure from the initial orbit and arrival at the final orbit at the optimum position is ensured. In certain instances, however, mission considerations preclude the usefulness of solutions which have negative initial or final coasts. For example, in the foregoing description of the AOA mission, the initial state vector was given at the Shuttle main engine cutoff in a launch trajectory, making it impossible for the mission designer to initiate the transfer at a position on the initial orbit previous to the input state vector. If the final state vector in the previous problem is changed to that in the third column of table I, a negative initial coast of 91.0 seconds is required as indicated by the data in column 1 of table III. Imposing the parameter inequality constraint developed in the appendix on the initial time yields the solution indicated in column 2. Note that the initial coast time is now 1.03 second and that, as expected, the  $\Delta V$  required for the transfer is higher. The constraint is stated such that the coast arc is only required to be non-negative, a 0-second coast arc can be expected. The actual constraint as implemented in the appendix is "hard" only in the limit of  $k \rightarrow \infty$ , so the program cannot satisfy the constraint precisely. A hard constraint is one in which the quantity being constrained may take on a value equal to the value of the constraint. In the example under discussion, the initial coast arc would have a 0-second duration if the constraint were hard.

TABLE III  
INEQUALITY CONSTRAINT EXAMPLE

		<u>Unconstrained</u>	<u>Constrained</u>
Engine switch			
time array, sec	$t_0$	0	0
	$t_1$	-90.9	1.03
	$t_2$	3.97	96.5
	$t_3$	2557.8	2350.2
	$t_4$	2602.8	2396.3
Costate		-.184	-.195
		.882	.888
		0	0
		-.427	-.413
		-.12	-.108
		0	0
Intermediate orbit			
Perigee altitude, n. mi.		46.7	48.2
Apogee altitude, n. mi.		109.1	108.0
$\Delta V_1$ , fps		151.9	152.8
$\Delta V_2$ , fps		72.8	74.6
$\sum \Delta V$ , fps		224.7	227.4

Altitude profiles for the unconstrained and constrained example AOA missions are illustrated in figures 2(b) and (c). The profiles are very similar. Note that the second burn arc occurs closer to apogee in the constrained solution.

### Synchronous Orbit Missions

Many of the satellite placement missions planned for the Shuttle require additional propulsion to achieve the required orbit. To provide the additional propulsion a general purpose rocket vehicle called a tug is being developed. Several designs are being considered. In an effort to save weight some of these designs entail the use of a rather small engine, which results in a low thrust-to-weight ratio. This sometimes complicates mission planning efforts to ensure that the tug will be used as efficiently as possible. One particularly severe mission, for which there are numerous payloads, is the placement of a satellite in a geosynchronous orbit. This mission is difficult because of the large altitude change and the large plane change ( $29^\circ$ ) required between the initial and final circular orbits. The altitude of a circular geosynchronous orbit is 19 323 n. mi. As a further example of the capability of OPBURN, this mission was chosen for solutions with vehicle thrust-to-weight ratios as low as 0.1. Solutions for the mission will include two- and three-burn profiles.

The geosynchronous satellite placement mission is initiated in a low-altitude circular orbit sized according to the capabilities of the Shuttle. For this example, a circular orbit of 150-n. mi. altitude was assumed. The initial state vector is given in table IV. For ease of input, a coordinate system was established so that the initial orbit was in the X-Y plane, and the line of intersection (i.e., the line of nodes)

TABLE IV

## EXAMPLE GEOSYNCHRONOUS ORBIT MISSION DATA

State vectors

	<u>Initial</u>	<u>Final</u>
Radius, ft	21 837 155.0	138 333 497.0
Right ascension deg	-90.0	180.0
Declination, deg	0	0
Velocity, fps	25 389.25	10 087.52
Flight-path angle, deg	0	0
Azimuth, deg	90.0	61.0

Vehicle characteristics

Initial weight, lb	100 000
Thrust, lb	30 000, 20 000, 10 000
Specific impulse, sec	420

of the initial and final orbit planes was along the X-axis (fig. 3). The final state vector, also given in table IV, corresponds to a circular orbit with an altitude of 19 323 n. mi. and at an inclination of  $29^\circ$  from the X-Y plane. Vehicle characteristics shown were chosen to produce vehicle thrust-to-weight ratios ( $T/w_T$ ) of 0.3, 0.2, and 0.1. The specific impulse selected is that of a proposed oxygen difluoride/methane propellant tug.

The two-burn mission profile consists of two thrust arcs. The first, which is centered approximately on the line of nodes, places the spacecraft into an elliptical transfer orbit with an apogee altitude approximately that of the desired final circular orbit. The second thrust arc, which occurs at the apogee of the transfer orbit, circularizes the spacecraft at the desired altitude. Each thrust arc concurrently performs a portion of the required plane change; in other words, the first thrust arc achieves a small part of the required plane change, and the second completes it. In the three-burn profile, the function of the first thrust arc in the two-burn profile is achieved by the first two thrust arcs. These thrust arcs are separated by approximately one revolution in an elliptical orbit and centered approximately on the same node. Each mission profile is illustrated in figure 4.

As in the previous example, an estimate of the engine switch times was provided and the costate estimation routine employed to produce a costate vector estimate based on the knowledge that all of the burns would be posigrade. These estimates for the control variables were then transferred to the  $\omega$  program for convergence to an estimate for the optimal control. The optimal control estimate from the  $\omega$  program was used as a starting iterate for the inverse-square program in the two- and three-burn cases.

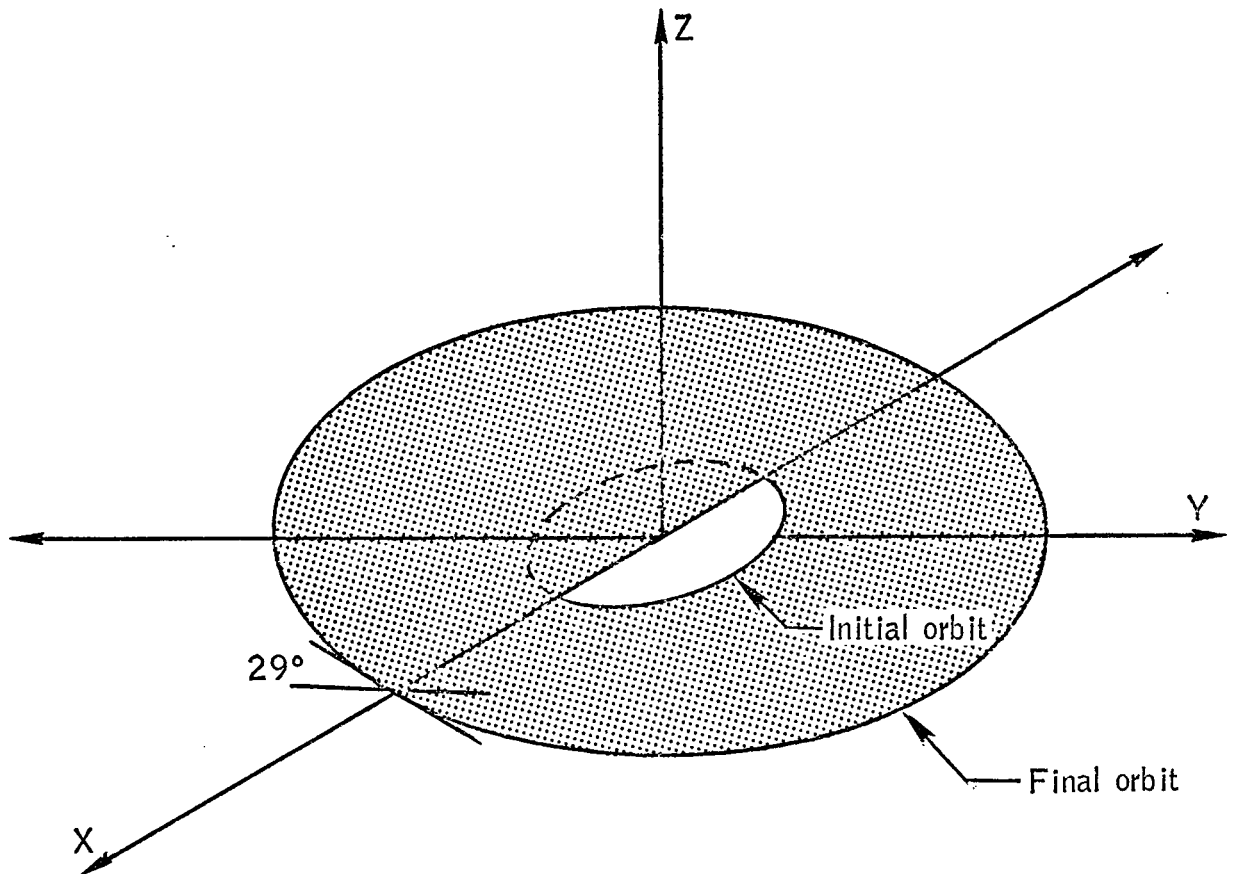


Figure 3.- Illustration of geosynchronous orbit mission  
Initial and final orbit geometry.

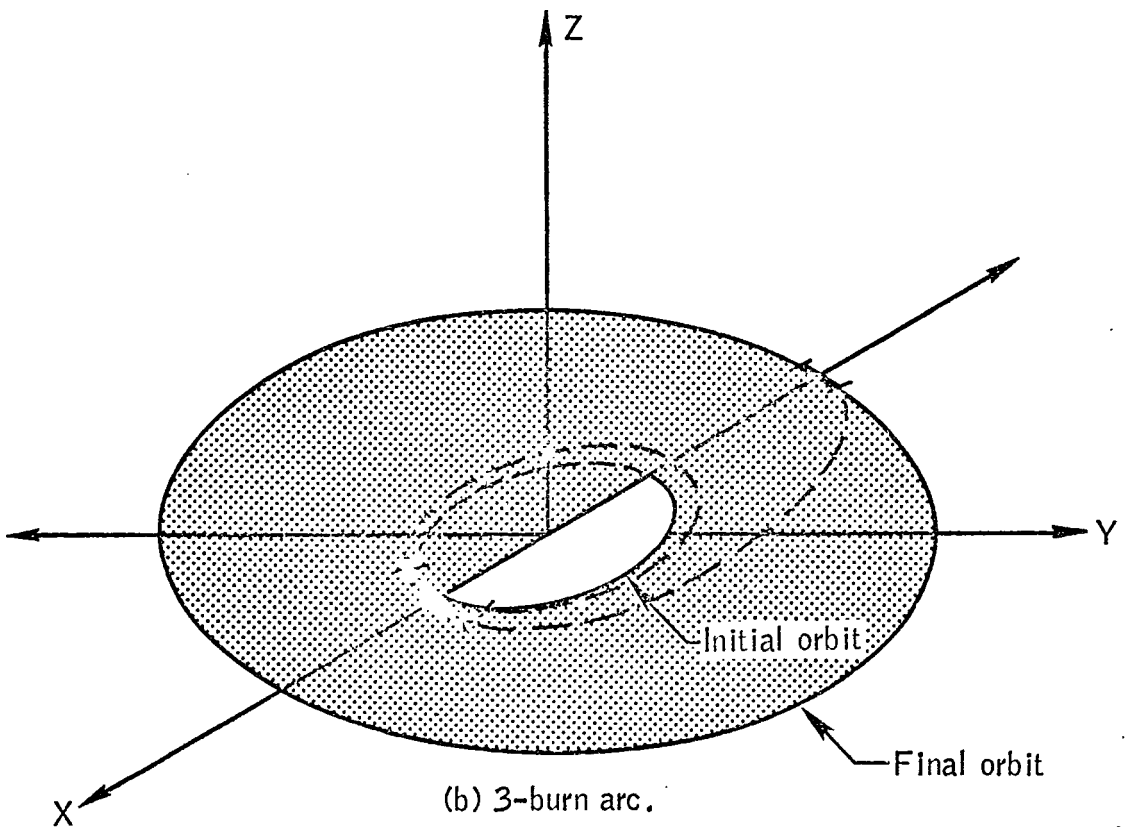
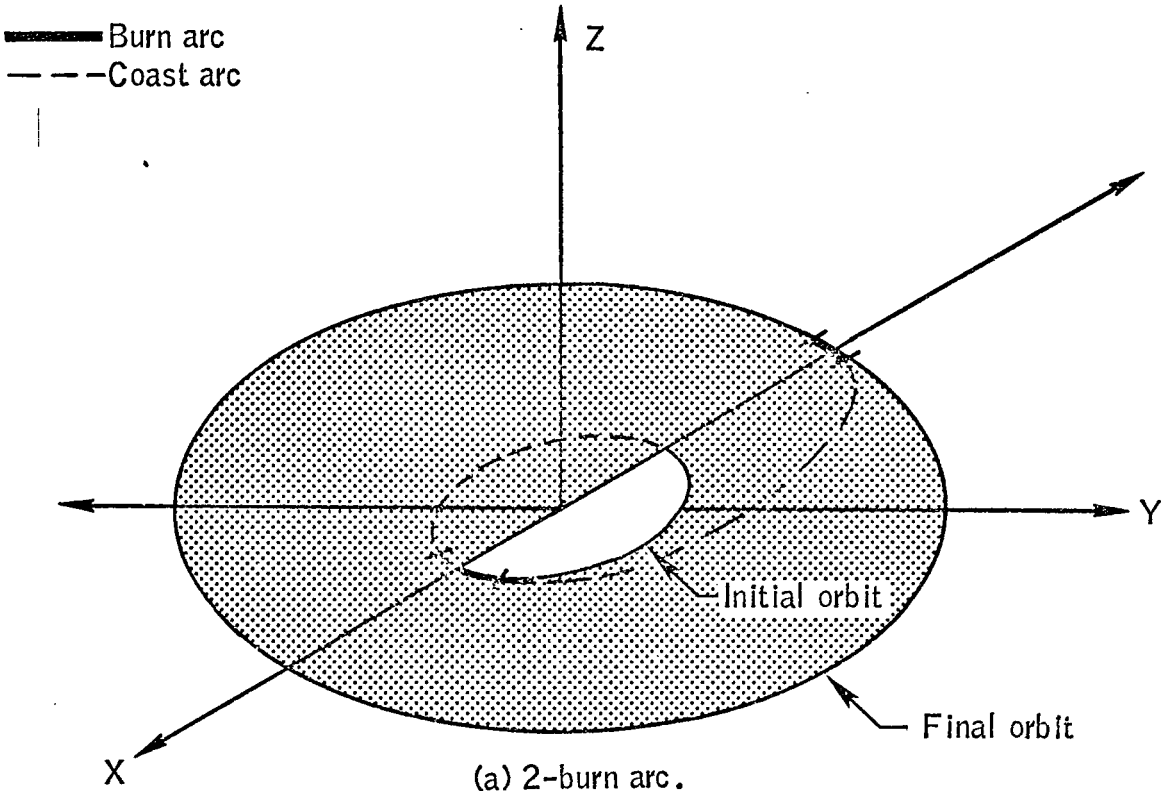


Figure 4. - Illustration of geosynchronous orbit mission profiles.

Parameters describing optimal two- and three-burn geosynchronous orbit missions for vehicles with a  $T/w_I$  of 0.3 are listed in table V. The time arrays listed in the initial estimate column were the estimates provided the program; the costates in those columns are produced by the costate estimation routine. The columns labeled " $\omega$  solution" give the values of parameters describing the solutions obtained from the  $\omega$  program. The values describing the solutions obtained from the full inverse-square program are listed in the columns labeled "inverse-square solution." The two three-burn solutions are in close agreement. This indicates that the gravity approximation in the  $\omega$  program is accurate in this case. The  $\omega$  solution to the two-burn problem does not agree with the inverse-square solution as well as the  $\omega$  solution to the three-burn problem. Note that the  $\Delta V$  requirement for the  $\omega$  solution is 45 fps higher than that found by the inverse-square program. All of the increase is required in the first thrust arc, which indicates that the gravity approximation does not have sufficient accuracy on that arc. Since the gravity approximation equation (24) is a linear function of position, the accuracy of the approximation on a thrust arc will depend on the altitude excursion of the vehicle in that arc.

Data describing the same missions for vehicles with a  $T/w_I = 0.2$  are given in table VI. Again there is acceptable agreement between the  $\omega$  and inverse-square solutions. Because of the lower  $T/w_I$ , longer thrust arcs are required to produce a given orbital change, so a larger altitude excursion results and the  $\omega$  approximation is less accurate for these solutions than when the  $T/w_I$  was 0.3. This fact is evident by examining

TABLE V  
 GEOSYNCHRONOUS MISSION SOLUTION PARAMETERS

( $T/w_I = 0.3$ )

		<u>No. of thrust arcs = 2</u>			<u>No. of thrust arcs = 3</u>		
		Initial estimate	$\omega$ solution	Inverse-square solution	Initial estimate	$\omega$ solution	Inverse-square solution
Engine switch time array, sec	$t_0$	0	0	0	0	0	0
	$t_1$	900	956	1 005	1 180	1 180	1 175
	$t_2$	1 650	1 591	1 637	1 520	1 518	1 514
	$t_3$	20 320	20 252	20 250	10 660	10 662	10 654
	$t_4$	20 600	20 522	20 521	10 950	10 953	10 944
	$t_5$				29 600	29 656	29 756
	$t_6$				29 880	29 928	29 848
Costate vector		0.362	0.699	0.691	1.14	0.680	0.687
		.227	.185	.202	-0.064	.219	.211
		0	-.0007	.0021	.529	.00023	.00035
		.452	.173	.189	-.075	.205	.645
		0	-.168	-.165	-.1	-.172	-.169
Intermediate orbits							
Perigee altitude, n. mi./		227/68 426	202/19 322	190/19 322	158/3450	156/3403	155/3420
apogee altitude, n. mi.					168/19 723	161/19 323	160/19 323

TABLE V

## GEOSYNCHRONOUS MISSION SOLUTION PARAMETERS - Concluded

$$(T/w_I = 0.3)$$

	<u>No. of thrust arcs = 2</u>			<u>No. of thrust arcs = 3</u>		
	Initial estimate	$\omega$ solution	Inverse-square solution	Initial estimate	$\omega$ solution	Inverse-square solution
$\Delta$ inclination, deg						
Burn 1	0	2.13	2.15	.8	1.16	1.17
Burn 2	0	26.87	26.85	.28	1.04	1.03
Burn 3				3.5	26.8	26.8
$\Delta V$ , fps						
Burn 1	10 376	8 183	8 133	3 762	3 741	3 752
Burn 2	7 621	5 868	5 864	4 323	4 339	4 325
Burn 3				6 112	5 880	5 883
$\Sigma \Delta V$ , fps	17 997	14 052	14 007	14 197	13 960	13 960

TABLE VI  
 GEOSYNCHRONOUS MISSION SOLUTION PARAMETERS  
 ( $T/w_I = 0.2$ )

		<u>No. of thrust arcs = 2</u>			<u>No. of thrust arcs = 3</u>		
		Initial estimate	$\omega$ solution	Inverse-square solution	Initial estimate	$\omega$ solution	Inverse-square solution
Engine switch time array, sec	$t_0$	0	0	0	0	0	0
	$t_1$	800	758	831	1 140	1 140	1 043
	$t_2$	1 800	1 723	1 788	1 725	1 726	1 618
	$t_3$	20 320	20 238	20 233	10 920	11 868	11 793
	$t_4$	20 540	20 636	20 634	11 340	12 235	12 165
	$t_5$				30 050	31 015	31 030
	$t_6$				30 460	31 418	31 437
Costate vector		1.05	0.636	0.695	1.10	0.696	0.691
		-.053	.093	.190	-.064	.104	.202
		0	0	0	0	.00006	-.000088
		-.05	.087	.179	-.601	.098	.189
		1.02	.742	.651	1.05	.686	.647
		0	-.167	-.16	0	-.151	-.165

TABLE VI

## GEOSYNCHRONOUS MISSION SOLUTION PARAMETERS - Concluded

$(T/w_I = 0.2)$

	<u>No. of thrust arcs = 2</u>			<u>No. of thrust arcs = 3</u>		
	Initial estimate	$\omega$ solution	Inverse-square solution	Initial estimate	$\omega$ solution	Inverse-square solution
Intermediate orbits						
Perigee altitude, n. mi./	311/24 200	255/19 322	241/19 322	171/3751	174/4372	168/4240
apogee altitude, n. mi.				223/20 130	207/19 322	175/19 326
$\Delta$ inclination, deg						
Burn 1	0	2.03	2.08	0	1.33	1.29
Burn 2	0	26.97	26.92	0	.87	.88
Burn 3					26.8	26.83
$\Delta V$ , fps						
Burn 1	8 745	8 329	8 225	3 977	4 423	4 326
Burn 2	3 017	5 857	5 858	4 226	3 756	3 779
Burn 3				5 995	5 864	5 879
$\Sigma \Delta V$ , fps	11 762	14 186	14 082	14 198	14 043	13 984

the characteristic velocity requirements for the two-burn solution in table VI. The  $\omega$  program indicates a  $\Delta V$  requirement 103 fps greater than the requirement found by the inverse-square program. All of this increased cost is required to accomplish the first thrust arc. In the three-burn case, the  $\omega$  solution requires a total of 59 fps more than in the inverse-square solution. The increased cost cannot be attributed as easily to any particular thrust arc due to the differences in the solutions. For example, the first thrust arc required 97 fps more in the  $\omega$  solution than in the inverse-square solution; however, the apogee of the first intermediate orbit is 132 n. mi. higher in the  $\omega$  solution. The transfer to that orbit would require a larger  $\Delta V$ .

Parameters describing two- and three-burn solutions to the geosynchronous orbit mission for vehicles with a  $T/w_I$  of 0.1 are listed in table VII. Data describing the inverse-square solution are provided only for the two-burn case. No inverse-square solution is provided for the three-burn solution because the  $\omega$  solution proved to be unsatisfactory as a starting iterate for the inverse-square program. Note the large difference between the  $\omega$  and inverse-square solutions in the two-burn case. The difference indicates the the  $\omega$  program solution has little value because of the inaccuracy of the gravity approximation, although the  $\omega$  program did converge given the time array shown and costate estimate produced by the costate estimation routine. Also, while the inverse-square solution did converge, the  $\omega$  solution was not suitable as a starting iterate in the inverse-square program. This was because the  $\omega$  solution produced a large initial error in boundary condition satisfaction in the inverse-square program and a large amount of computer time was required to attain convergence.

TABLE VII

## GEOSYNCHRONOUS MISSION SOLUTION PARAMETERS

 $(T/w_I = 0.1)$ 

	<u>No. of thrust arcs = 2</u>			<u>No. of thrust arcs = 3</u>	
	Initial estimate	$\omega$ solution	Inverse-square solution	Initial estimate	$\omega$ solution
Engine switch time array,	$t_0$	0	0	0	0
sec	$t_1$	425	641	304	1 076
	$t_2$	2 375	1 567	2 294	2 050
	$t_3$	20 360	20 628	20 231	9 872
	$t_4$	21 150	21 313	21 001	10 850
	$t_5$			29 162	29 163
	$t_6$			29 947	29 948
Costate vector		1.02	0.901	0.710	1.09
		-.032	-.375	.148	-.063
		0	-.0007	.001	0
		-.029	-.352	.139	-.059
		1.01	.962	.659	1.04
		0	-.218	-.143	0
					-.3 $\times 10^{-6}$
					-.0144
					1.1
					-.200

TABLE VII

## GEOSYNCHRONOUS MISSION SOLUTION PARAMETERS - Concluded

$(T/w_I = 0.1)$

	<u>No. of thrust arcs = 2</u>			<u>No. of thrust arcs = 3</u>	
	Initial estimate	$\omega$ solution	Inverse-square solution	Initial estimate	$\omega$ solution
Intermediate orbits					
Perigee altitude, n. mi./	795/11 432	867/19 321	520/19 321	232/3024	220/3005
apogee altitude, n. mi.				396/19 470	350/19 321
$\Delta$ inclination, deg					
Burn 1	0	1.48	1.84	0	0.98
Burn 2	0	27.52	27.16	0	1.19
Burn 3				0	26.83
$\Delta V$ , fps					
Burn 1	8 934	10 081	8 675	3 565	3 569
Burn 2	5 844	5 696	5 776	4 880	4 879
Burn 3				5 804	5 810
$\Sigma \Delta V$ , fps	14 278	15 777	14 451	14 251	14 259

The performance data for the geosynchronous orbit missions were plotted as a function of  $T/w_I$  (fig. 5) to illustrate the effects of lower thrust-to-weight ratios and the benefits of increasing the number of thrust arcs used to accomplish the mission. The graph indicates that there is a 500-fps penalty for reducing  $T/w_I$  from 0.3 to 0.1 when a two-burn transfer is used. The  $\omega$  solution curve for three-burn transfers indicates a penalty of 300 fps for reducing  $T/w_I$  from 0.3 to 0.1. Some of that penalty is caused by the gravity assumption in the  $\omega$  program, as is evident by comparing the penalties indicated for reducing  $T/w_I$  from 0.3 to 0.2. The  $\omega$  solution curve shows an 83-fps penalty, whereas the inverse-square solution curve indicates a penalty of only 24 fps. The three  $\omega$  solutions for  $T/w_I = 0.1$  show that a definite though diminishing performance improvement is possible by increasing the number of thrust arcs.

In all cases investigated the costate estimation routine produced estimates for the costate vector from which the  $\omega$  program converged. In some cases a more accurate time estimate was available than in others. This resulted in fewer iterations being required by the  $\omega$  program. The time estimates given in tables V, VI, and VII do not necessarily reflect the accuracy required by the program. They were simply the best available to the author.

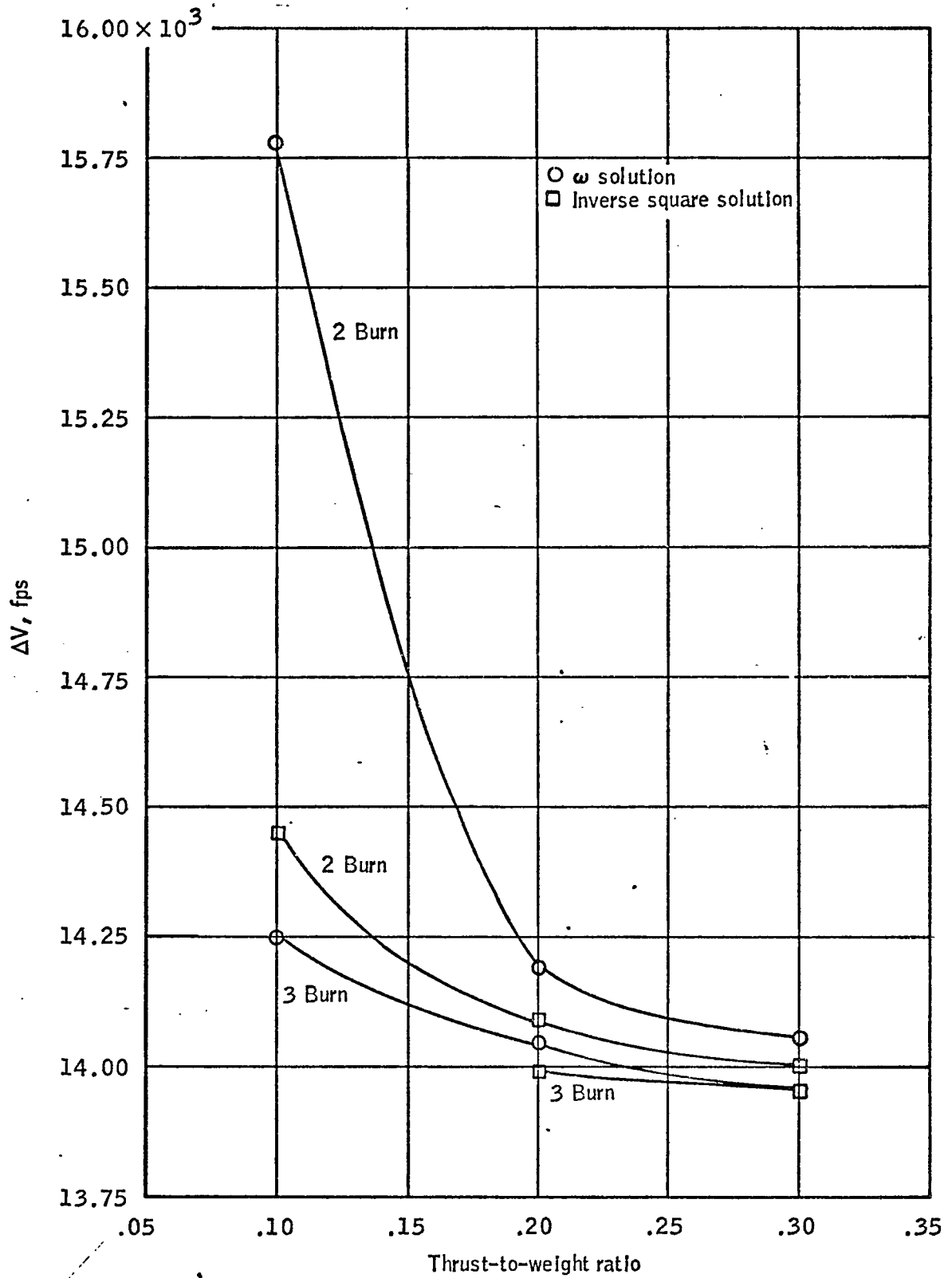


Figure 5.- Performance comparison for various geosynchronous orbit transfers.

## Chapter VI

## CONCLUSIONS AND RECOMMENDATIONS

A program is now available for optimal analysis of multiple burn space missions. The program does not require that the user have knowledge of optimal control principles. This is the result of the development of the costate estimation subroutine which requires that the user input only physical quantities that can be identified and estimated. Through the use of the  $\omega$ /inverse-square combination the author has become confident that the solutions produced by the  $\omega$  program are accurate, so that the inverse-square phase of OPBURN is not generally required. It is retained in OPBURN as a valuable program for solution verification of particular missions, especially when a new class of solutions is being produced.

Although the program produces useful results, a number of improvements and additions are suggested:

1. The addition of the capability to segment thrust arcs in the  $\omega$  program, reinitializing the gravity approximation each time. This would increase the accuracy of the  $\omega$  program and reduce or eliminate the inaccuracies noted in the geosynchronous missions due to large altitude excursions on long thrust arcs. Through the use of a segmented solution, the range of cases for which the  $\omega$  solution would be a suitable starting iterate should be increased (e.g., the three-burn geosynchronous mission with  $T/w_I = 0.1$ ).

2. The addition of parameter inequality constraints on the switch times in the inverse-square program. This would make the  $\omega$ /inverse-square combination compatible for a wider range of cases.

3. Development of an interactive program for mission planner use which would accept his input data, call the costate estimation program, and display the resulting trajectory. With such a program the mission planner could interactively determine thrust arc placement and size so that the resulting trajectory could be transferred to an execution of the OPBURN program with a greater chance of convergence to the desired answer.

## APPENDIX - PARAMETER INEQUALITY CONSTRAINTS

In order to restrict the  $\omega$  program so that coast and burn arcs of negative time duration are prohibited, it is necessary to implement an inequality constraint. The algorithm provided in the  $\omega$  program (ref. 8) was modified to include an inequality constraint by the penalty function approach. The penalty function described in ref. 11 was selected because it has the property that it and all of its derivatives are continuous. The penalty function is given by

$$J_p(\alpha) = \sum_{i=1}^m d_i e^{[1-(1+\alpha_i)^k]} \quad (A-1)$$

where  $\alpha$  is the  $m$  vector of parameters,  $d$  is a penalty constant, and  $k$  is some integer.

Given the vector function  $f(\alpha)$ , we wish to find  $\alpha$  such that  $f(\alpha) = 0$ , subject to the constraints that some or all of the parameters  $\alpha_i$  remain non-negative. First form the function

$$J'(\alpha) = J(\alpha) + J_p(\alpha) \quad (A-2)$$

where

$$J(\alpha) = \frac{1}{2} f(\alpha)^T W_y f(\alpha) \quad (A-3)$$

and expand it in a Taylor series to second-order terms about  $\alpha^*$ , the constrained solution to  $f(\alpha) = 0$ :

$$\begin{aligned}
J'(\alpha) &= J(\alpha^*) + J_p(\alpha^*) + \left[ \frac{\partial J}{\partial \alpha} \Big|_{\alpha^*} + \frac{\partial J_p}{\partial \alpha} \Big|_{\alpha^*} \right] (\alpha - \alpha^*) \\
&+ \frac{1}{2} (\alpha - \alpha^*)^T \left[ \frac{\partial^2 J}{\partial \alpha^2} \Big|_{\alpha^*} + \frac{\partial^2 J_p}{\partial \alpha^2} \Big|_{\alpha^*} \right] (\alpha - \alpha^*)
\end{aligned} \tag{A-4}$$

At  $\alpha^*$ ,

$$\frac{\partial J}{\partial \alpha} \Big|_{\alpha^*} + \frac{\partial J_p}{\partial \alpha} \Big|_{\alpha^*} = 0 \tag{A-5}$$

so that

$$J'(\alpha) = J(\alpha^*) + J_p(\alpha^*) + \frac{1}{2} (\alpha - \alpha^*)^T \left[ \frac{\partial^2 J}{\partial \alpha^2} \Big|_{\alpha^*} + \frac{\partial^2 J_p}{\partial \alpha^2} \Big|_{\alpha^*} \right] (\alpha - \alpha^*) \tag{A-6}$$

Using this  $J'$ , find the gradient

$$G'(\alpha) = \frac{\partial J'}{\partial \alpha} = (\alpha - \alpha^*)^T \left[ \frac{\partial^2 J}{\partial \alpha^2} \Big|_{\alpha^*} + \frac{\partial^2 J_p}{\partial \alpha^2} \Big|_{\alpha^*} \right] \tag{A-7}$$

It is now possible to solve for  $\Delta\alpha$  by assuming that the second-order terms vary slowly,

$$\Delta\alpha = \alpha^* - \alpha = - \left[ \frac{\partial^2 J}{\partial \alpha^2} + \frac{\partial^2 J_p}{\partial \alpha^2} \right]^{-1} G'(\alpha)^T \tag{A-8}$$

All that remains is to determine  $G'(\alpha)$  and  $\frac{\partial^2 J}{\partial \alpha^2}$ . Differentiating equation (A-2) yields

$$G'(\alpha)^T = \frac{\partial J^T}{\partial \alpha} + \frac{\partial J_p^T}{\partial \alpha} = \frac{\partial f^T}{\partial \alpha} W_y f + \frac{\partial J_p^T}{\partial \alpha} \tag{A-9}$$

and differentiating equation (A-3) twice gives

$$\frac{\partial^2 J}{\partial \alpha^2} = \frac{\partial f^T}{\partial \alpha} W_y \frac{\partial f}{\partial \alpha} + f^T W_y \frac{\partial^2 f}{\partial \alpha^2} \tag{A-10}$$

which contains the undesirable term  $\frac{\partial^2 f}{\partial \alpha^2}$ . To circumvent the complex computation involved in the last term, it is approximated by

$$f^T W_y \frac{\partial^2 f}{\partial \alpha^2} = \gamma W_x \quad (\text{A-11})$$

so that

$$\Delta \alpha = - \left( \frac{\partial f}{\partial \alpha} W_y \frac{\partial f}{\partial \alpha} + \frac{\partial^2 J_p}{\partial \alpha^2} + \gamma W_x \right)^{-1} \left( \frac{\partial f}{\partial \alpha} W_y f + \frac{\partial J_p}{\partial \alpha} \right)^T \quad (\text{A-12})$$

Note from equation (A-1) that  $J_p(\alpha)$  is a summation of terms each of which is a function of only one parameter. Because of this property, the gradient  $\frac{\partial J_p}{\partial \alpha}$  is a row vector with  $m$  terms, and each term,  $\frac{\partial J_p}{\partial \alpha_i}$ , is a function of the  $i$ th parameter only. Proceeding to the second derivative,  $\frac{\partial^2 J_p}{\partial \alpha^2}$ , note that it is an  $m$ -by- $m$  diagonal matrix with the  $i$ , $i$ th element a function of the  $i$ th parameter only.

In the  $\omega$  program, the vector,  $\alpha$ , is composed of six costate components and a  $2n+1$  array of times. Since it is desired to constrain the times only,  $d_i = 0$ ,  $i = 1, \dots, 6$ . The value for the remaining  $d_i$  will be set to

$$d = 10^j C \quad (\text{A-13})$$

where  $C$  is the value of  $J'(\alpha)$  of the previous iteration. Initially,  $j=2$  with provision for its increase should the constraint be violated. The value of  $k$  in (A-1) is nominally set to 2501, which produces a minimum arc duration of less than 1 second for each time constrained. The odd number 2501 is required to eliminate symmetry from equation (A-1). If the penalty function is allowed to be symmetric, then the possibility exists for a solution which violates the constraint but for which no penalty is assessed (i.e.,  $\alpha_i < -2$ ).

The two weighting matrices,  $W_x$  and  $W_y$ , will normally be identity matrices. However, they can be defined as required for special situations so long as  $W_y$  is positive definite. An algorithm exists in the  $\omega$  program to modify  $W_y$  so that the tolerance to which optimality conditions are satisfied is increased. This is provided because it may not be possible to satisfy the optimality conditions completely in cases in which the first and/or the last coast arcs are constrained.

## REFERENCES

1. Jezewski, D. J. and Rozendaal, H. L., "An Efficient Method for Calculating Optimal Free-Space N-Impulse Trajectories," AIAA Journal, Vol. 6, No. 11, November 1968.
2. McAdoo, S. F. and Funk, J., "An Earth Departure Technique for Use in Manned Interplanetary Missions Using the NERVA Engine," AAS 70-039, presented at the AAS/AIAA Astrodynamics Conference, June 1970.
3. Johnson, I. L. and Kamm, J. L., "Near Optimal Shuttle Trajectories Using Accelerated Gradient Methods," AAS/AIAA Paper Number 328, presented at the AAS/AIAA Astrodynamics Specialists Conference, August 1971.
4. Brown, K. R.; Harrold, E. F.; and Johnson, G. W.; "Rapid Optimization of Multiple-Burn Rocket Flights," NASA CR-1430, Prepared by International Business Machines Corp., Cambridge, Mass., September 1969.
5. Tarbet, J. D., "Optimum Continuous Control by a Method of Parameterization," Ph.D. Dissertation, University of Houston, August 1971.
6. Robbins, H. M., "An Analytical Study of the Impulsive Approximations, AIAA Journal, Vol. 4, No. 8, August 1966.
7. Jezewski, D. J., "N-Burn Optimal Analytic Trajectories," AIAA Journal, Vol. 11, No. 10, October 1973.
8. Goodyear, W. H., "Completely Closed-Form Solution for Coordinates and Partial Derivatives of the Two-Body Problem," The Astronomical Journal, Vol. 70, No. 3, April 1965.
9. Armstrong, E. S., "A Combined Newton-Raphson and Gradient Parameter Correction Technique for Solution of Optimal-Control Problems," NASA TR R-293 dated October 1968.

10. Jezewski, D. J., "Optimal Analytic Multiburn Trajectories," AIAA Journal, Vol. 10, No. 5, May 1972.
11. Jezewski, D. J., and Faust, N. L., "Inequality Constraints in Primer-Optimal, N-Impulse Solutions," AIAA Journal, Vol. 9, No. 4, April 1971.